Probing conformational dynamics of an enzymatic active site by an in situ single fluorogenic probe under piconewton force manipulation

Nibedita Pal[a], Meiling Wu[a], and H. Peter Lu[a,1]

[a]Department of Chemistry, Center for Photochemical Sciences, Bowling Green State University, Bowling Green, OH 43403

Edited by Hans Frauenfelder, Los Alamos National Laboratory, Los Alamos, NM, and approved November 15, 2016 (received for review August 11, 2016)

Unraveling the conformational details of an enzyme during the essential steps of a catalytic reaction (i.e., enzyme–substrate interaction, enzyme–substrate active complex formation, nascent product formation, and product release) is challenging due to the transient nature of intermediate conformational states, conformational fluctuations, and the associated complex dynamics. Here we report our study on the conformational dynamics of horseradish peroxidase using single-molecule multiparameter photon time-stamping spectroscopy with mechanical force manipulation, a newly developed single-molecule fluorescence imaging magnetic tweezers nanoscopic approach. A nascent-formed fluorogenic product molecule serves as a probe, perfectly fitting in the enzymatic reaction active site for probing the enzymatic conformational dynamics. Interestingly, the product releasing dynamics shows the complex conformational behavior with multiple product releasing pathways. However, under magnetic force manipulation, the complex nature of the multiple product releasing pathways disappears and more simplistic conformations of the active site are populated.

enzymatic conformational dynamics | magnetic tweezers | mechanical force manipulation | enzymatic product releasing | fluorogenic substrate

Enzymes are capable of enhancing biological reaction activity by millions or even billions of times (1). A typical enzymatic turnover cycle involves multiple steps: substrate (S) binding to the active site of the enzyme (E) in forming an enzyme–substrate complex E+S→[E•S]; enzymatic reaction converting substrate to nascent product (P), [E•S]→[E•P]; and product releasing from the enzyme active site, [E•P]→E+P, which completes an enzymatic reaction turnover (2–4). In recent years, it has been widely identified that conformational dynamics plays a crucial role in regulating enzymatic reactions (2, 4–7). The advent of site-specific mutagenesis, single-molecule (SM) spectroscopic technique, and molecular dynamics simulations have demonstrated complex dynamics involving multiple conformational states during a catalytic cycle (4, 5, 7–13). Fundamentally, not only the enzymatic active site conformational dynamics but also the overall conformational fluctuation dynamics of the protein matrix, providing the required entropy, enthalpy, and corresponding energy landscape, has a profound impact on an enzyme to ultimately possess the power of enhancing reaction rates. Nevertheless, capturing an individual snapshot of each intermediate conformational step remains challenging, mainly due to the transient nature of those intermediate structures, inadequacy of the conventional structure analysis methods to seize those fluctuating structures, and lack of molecular probes that can specifically report the active site environment at each step of an enzymatic reaction. More often than not, the rate-limiting step is the product release from the active site (14). However, a thorough and comprehensive picture of the product release mechanism is still insufficient, mostly due to the complexity and inhomogeneity of the enzymatic dynamics. For example, by what exact mechanism a product exits the active site and the energetically preferential configurations of an enzyme to release the product are still not clear. Few studies have tried to address these questions and related effects on other macroscopic parameters directly through experimental approaches (9, 15–19). We recently reported that horseradish peroxidase (HRP) can involve multiple intermediate conformational states and pathways during product releasing, and a significant pathway is that the product molecules are spilled out from the enzymatic reaction site; however, releasing the product molecules through a loosely bound enzyme-product state and an open active site remain parallel product releasing pathways (9). Further, very recently our group has reported that HRP retains a significant amount of its activity even under conformational perturbations (20). Here, we aim to systematically characterize not only the mechanism and dynamics involved in product release of HRP but also the complex conformational dynamics involved in each step of a catalytic cycle by directly manipulating the reaction coordinates. We further extended our study and applied our newly developed SM approach of actively manipulating the reaction coordinates using combined SM time-resolved photon time-stamping spectroscopy and magnetic tweezers to understand the effect of conformational perturbation on the conformational dynamics and mechanism of enzymatic product release.

The biological function of an enzyme is presumably followed in real time by using mainly three kinds of fluorescent reporter molecules: (*i*) intrinsic fluorescent residues (e.g., tryptophan or tyrosine), (*ii*) site-specific labeling, and (*iii*) fluorogenic substrate (8, 11, 21). Application of fluorogenic substrate (nonfluorescent) is a direct approach to follow enzymatic reaction turnovers as it gets converted into a fluorescent product molecule by the enzyme. As the product molecule quickly exits the detection volume within

Significance

The exploration of the internal conformational fluctuation dynamics of an enzyme during a catalytic event can have significant implications in the field of enzymology. How an enzyme modulates its conformations under mechanical perturbation while still retaining its activity to a significant extent can be of particular interest in the area of protein engineering. Using single-molecule total internal reflection fluorescence microscopy-guided confocal spectroscopy combined with magnetic tweezers we have interrogated the conformational dynamics of horseradish peroxidase enzyme. We have identified the presence of complex conformations during the product releasing step. However, the complexity is narrowed or even eliminated when the enzyme is deformed or unfolded under magnetic pulling force.

Author contributions: H.P.L. designed research; N.P. and M.W. performed research; H.P.L. contributed new reagents/analytic tools; N.P., M.W., and H.P.L. analyzed data; and N.P., M.W., and H.P.L. wrote the paper.

The authors declare no conflict of interest.

This article is a PNAS Direct Submission.

[1]To whom correspondence should be addressed. Email: hplu@bgsu.edu.

This article contains supporting information online at www.pnas.org/lookup/suppl/doi:10.1073/pnas.1613404114/-/DCSupplemental.

microseconds it provides a direct readout of enzymatic reactions with single turnover resolution (5, 8, 9, 22–24). Additionally, fluorescent product molecules are produced continuously in turnover cycles and this eliminates the negative impact of photobleaching, and thereby long time trajectories from a single enzyme can be recorded (8, 9). In this work, we extend the SM fluorogenic assay and imaging analysis to a new dimension by combing the total internal reflection fluorescence microscopy (TIRFM)-guided confocal time-resolved SM photon time-stamping spectroscopic approach and the SM fluorogenic assay combined with magnetic tweezers force manipulation of molecular conformations: We used the nascent formed fluorescent product as an in situ probe to study the active site conformational fluctuation dynamics during the enzymatic reaction from the moment the product incipiently formed to the releasing of the fluorescent product from the active site (9, 20, 25). It is a conceptual and technical advancement to use a nascent-formed fluorogenic product molecule serving as a probe for enzymatic reaction active site with perfectly fitted position with the critical molecular interactions without perturbing the active site as in the case of site-specific labeling. Furthermore, magnetic tweezers give us the edge over chemical denaturation by introducing conformational perturbation in a noninvasive and controlled way (20, 26), that is, we are able to deform the enzymatic conformations under enzymatic conditions, which is beyond the conventional protein structure denature assays that are carried out under chemical conditions, such as pH, electrolytes, and chemical denaturants, which are not physiological enzymatic reaction conditions.

Results

HRP is a 44-kDa monomeric metalloenzyme containing a heme prosthetic group and each substrate turnover is produced from a single catalytic cycle (27, 28). HRP oxidizes both organic and inorganic compounds in the presence of hydrogen peroxide (H_2O_2) as an oxidizing agent (28–30). We have used Amplex Red (10-acetyl-3,7-dihydroxyphenoxazine) as nonfluorescent substrate, which is converted into highly fluorescent resorufin by HRP in the presence of H_2O_2 (Fig. 1*A*) (23).

We used TIRFM to pinpoint spatially randomly located enzymes from the stochastic on–off fluorescence signals originating from catalytic cycles (Fig. 1 *B* and *C*). Successively using the confocal time-resolved SM photon time-stamping technique, we followed enzymatic turnover events for two different polarizations, vertical and parallel with respect to the excitation light polarization (Fig. 1 *D* and *E*) (see *Supporting Information* for details). In an SM photon time-stamping measurement, for each detected photon (here each data point in Fig. 2*E*) two parameters are recorded: chronic arrival time (t) and delay time between the photo excitation and each emitted photon (Δt) (31). The histogram of the delay times (Δt) gives a typical SM fluorescence lifetime (Fig. 1*E*) and the intensity trajectory is calculated from the distribution of arrival time (t) within a given bin time (Fig. 1*F, Lower*). Further, from the intensity trajectories in two different polarizations, rotational anisotropy can be calculated (Fig. 1*F, Upper*). Simultaneous measurements of photon chronic arrival time and delay time along with rotational anisotropy improve the resolution of detection of individual species and provide rich information about the properties of a fluorophore and its surrounding environment (9, 31–36). In this regard our study is unique and advanced in interrogating the product-releasing mechanism and associated conformational dynamics. In our assay, HRP was tethered to the glass coverslip according to Fig. 1*A* (see *Supporting Information* for details). In previous reports, typically ~100 nM substrate and from micromolar to

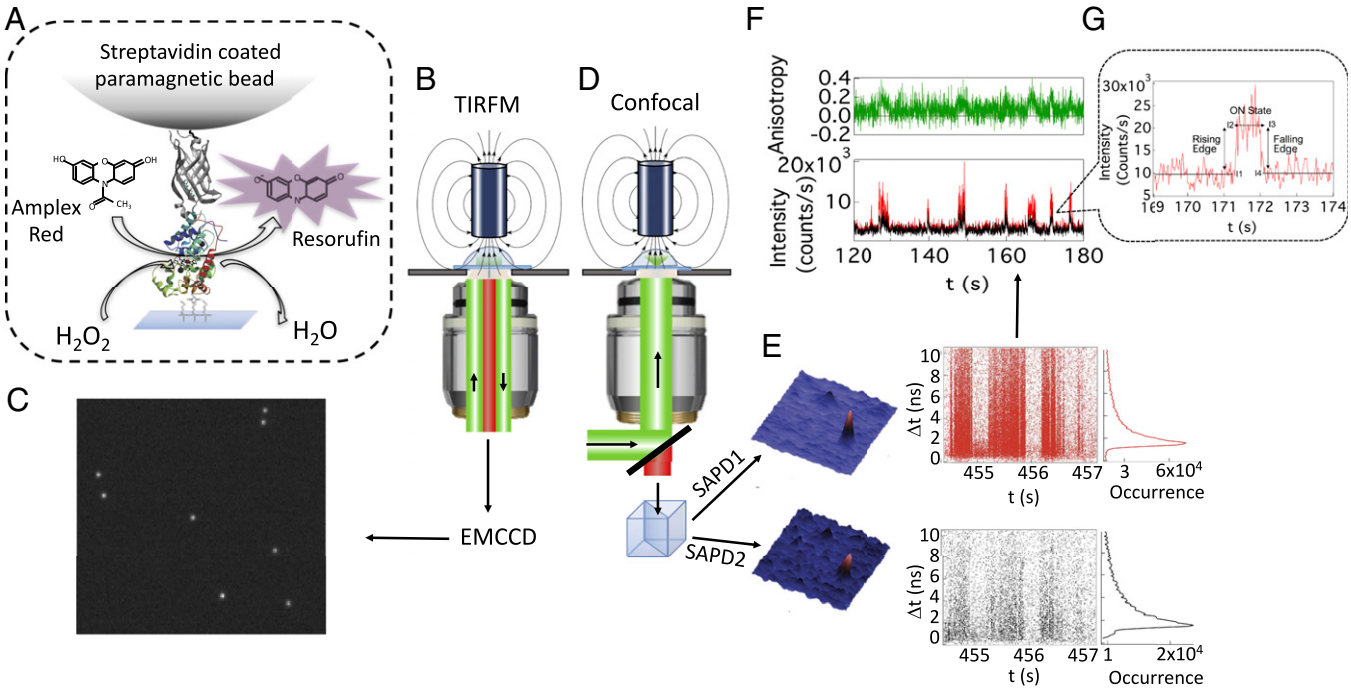

Fig. 1. Conceptual representation of our system and analysis method. (*A*) Single HRP enzyme is immobilized on a modified glass coverslip at one end and tethered to a paramagnetic bead at the other end through biotin–streptavidin linking. A magnetic field of ~2,000 Gauss at ~2 mm is applied to 1-μm-diameter paramagnetic beads to generate ~2 pN of pulling force on the beads and hence to the enzyme molecules (*Supporting Information*). (*B*) Schematic of wide-field excitation in TIRFM under an applied magnetic field. (*C*) Typical snapshot of an image from an electron multiplying CCD (EMCCD). (*D*) Schematic of the confocal microscope under an applied magnetic field. (*E*) Fluorescence confocal images collected in two polarization components from the single photon avalanche photodiodes (SAPD1 and SAPD2) and corresponding typical raw data of SM photon time stamping. (*F*) Intensity and anisotropy trajectories calculated from time-stamping data. (*G*) The rising edge, ON state, and the falling edge of a catalytic event.

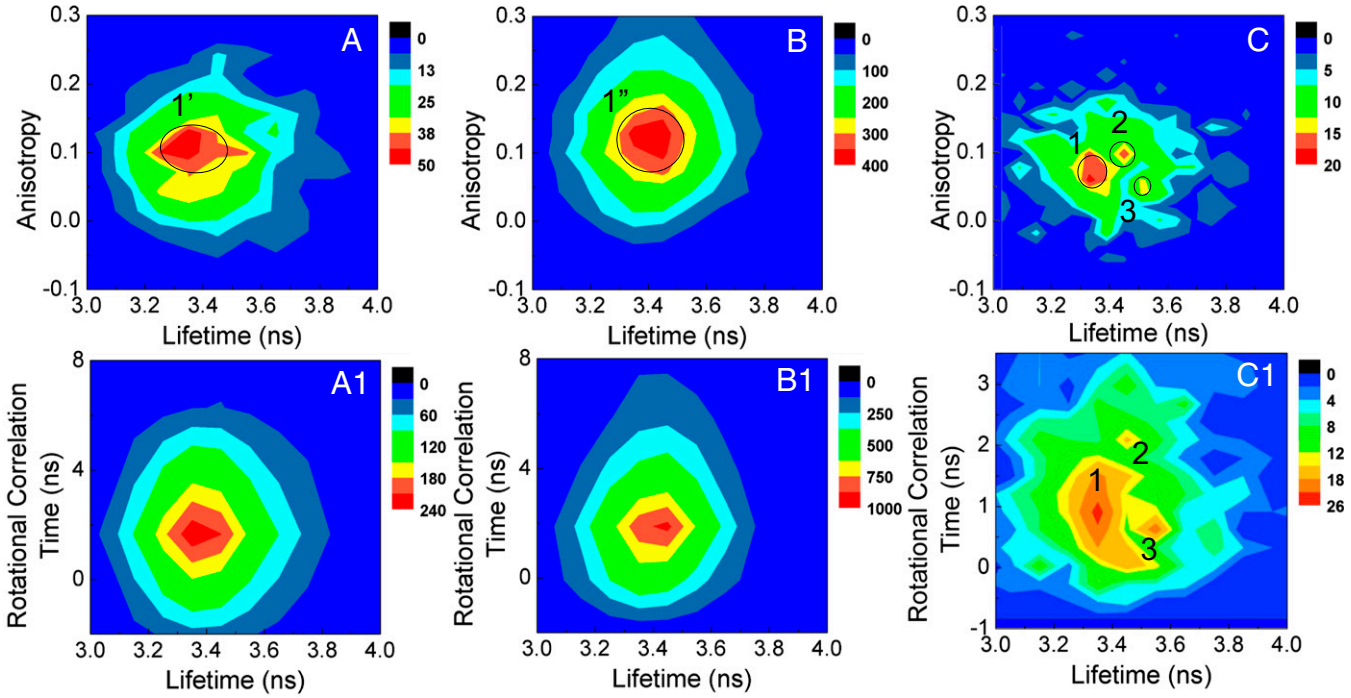

Fig. 2. Two-dimensional joint distribution of anisotropy and lifetime (*Upper*) and rotational correlation time and lifetime (*Lower*) calculated from 281 catalytic turnovers. Two-dimensional joint distribution of anisotropy and lifetime at (*A*) the rising edge, (*B*) ON state, and at (*C*) the falling edge. Two-dimensional joint distribution of rotational correlation time and lifetime at (*A1*) the rising edge, (*B1*) ON state, and (*C1*) the falling edge.

millimolar concentrations of H_2O_2 have been used to avoid enzymatic side reactions, autoxidation, and photooxidation of nonfluorescent substrate to fluorescent product (5, 24, 37, 38). The reaction solution in the current work contains 200 nM Amplex Red and 2 mM H_2O_2. A low turnover rate (~0.1–0.3 s^{-1}) is recorded due to the low substrate concentration. Additionally, only those isolated events with a high fluorescence photon count (>1,000 photons over the entire catalytic event) are considered and analyzed subsequently. The low turnover rate helps us to identify single enzymatic events distinctly, which remains the main focus of this study. However, we cannot completely exclude the effect of steric hindrance of tethered enzymes on turnover rate (39).

Fig. 1*F* shows a portion of anisotropy trajectory and the corresponding intensity trajectories in two polarization channels. Single enzymatic events can be detected as photon bursts with amplitudes above the background noise. The fluorescence signal from the product can be detected only when it is still confined within the active site. The microsecond diffusion time of product fluorescent molecule essentially eliminates the possibility of acquiring a fluorescence signal from diffusing fluorescent molecules (40). As evident from Fig. 1*F*, the anisotropy fluctuates around zero between consecutive fluorescent bursts or events. During a catalytic event, anisotropy increases drastically to a higher value. The higher anisotropy value signifies that during a catalytic event the fluorescent product exhibits relatively confined motion inside the active site of the enzyme. The anisotropy fluctuations can arise from the dynamic conformational fluctuation of the protein matrix and nearby local environment. Aromatic substrates form a stable 1:1 complex with HRP through hydrophobic interactions and hydrogen bonds involving the amino acid residues arginine, histidine, and proline (27, 28). The rigid interaction of resorufin with active-site residues through hydrogen bonding and hydrophobic interaction prevents the product from rotating freely inside the active site. The relatively confined rotation of fluorescent product is reflected in the measured high anisotropy, which also reflects the conformational dynamics of active site, specifically the solvent-exposed heme prosthetic group (9). To identify the specific nature of enzyme–substrate and enzyme–product interactions at the active site we have divided a catalytic event into three parts probed from the signals (Fig. 1*G*): the rising edge, ON state, and falling edge. The rising edge corresponds to the nascent product formation, which is the onset of an enzymatic turnover, ON time represents the duration when the product is still confined to the active site, and falling edge corresponds to the moment just before the product is released from the active site of the enzyme (*Supporting Information*). Dividing a catalytic event into different parts gives us insight about how the active-site conformation evolves with time as the reaction proceeds along the reaction coordinate.

To investigate in detail, we have plotted the 2D joint distribution of lifetime (τ_f) and anisotropy (r) (32, 41). Fig. 2 *A–C* shows the 2D joint distribution of fluorescence lifetime and anisotropy at the rising edges, during the ON states, and at the falling edges, respectively, from 281 catalytic events. SM fluorogenic product lifetime is calculated as the average delay times of all of the photons in 20-ms bin times for both polarizations. Fig. 2*A* clearly shows only one domain exists (domain 1′) in anisotropy and lifetime joint distribution at the rising edge. Domain 1′ centers around $\tau_f = 3.3 \pm 0.2$ ns and $r = 0.11 \pm 0.04$. All of the error bars are calculated as two SDs so that 95% of the data fall within two SDs from the mean and the SDs for all of the domains are calculated from the data that fall within the black circles. The similar conformation continues to persist along the reaction coordinate because only one domain (domain 1′′) is present during ON state centering on $\tau_f = 3.4 \pm 0.1$ ns and $r = 0.12 \pm 0.06$, similar as domain 1′ (Fig. 2*B*). This result strongly suggests that the active site conformation populated during the rising edge (i.e., when the nascent product is formed) continues to persist as the reaction proceeds. The large SDs of domain 1′ and 1′′ represent the large-scale conformational motions involved. Interestingly, the 2D joint distribution of falling edge (Fig. 2*C*) exhibits three distinct domains (domains 1, 2, and 3). The

presence of multiple distinct domains reveals that multiple distinct conformations of the active site of HRP are populated during the time the product resorufin is released from the active site. Domain 1 is centered on $\tau_f = 3.3 \pm 0.1$ ns and $r = 0.07 \pm 0.04$, domain 2 is centered at $\tau_f = 3.5 \pm 0.04$ ns and $r = 0.10 \pm 0.04$, and domain 3 is centered on $\tau_f = 3.5 \pm 0.04$ ns and $r = 0.05 \pm 0.02$. We further calculated the corresponding rotational correlation time (τ_r) for all of the domains (*Supporting Information*). Domain 1′ of the rising edge is centered on 1.8 ns, which has a τ_r similar to domain 1′′ of the ON state ($\tau_r = 2.0$ ns). In the falling edge, the corresponding τ_r for domains 1, 2, and 3 are 0.9, 1.5, and 0.6 ns, respectively. It is interesting to observe that in the falling edge domain 2 has a τ_r comparable to that of at the rising edge and ON state. Resorufin has a rotational correlation time of ∼0.1 ns in water (42). The higher anisotropy and τ_r (1.5 ns) in domain 2 correspond to a confined environment or tightly bound state for resorufin. Domains 1 and 3 have lifetime values similar to those of other domains but much smaller anisotropy and hence a faster rotational correlation time, which may represent a much looser state of the HRP active site. Loose enzyme–product states present in domains 1 and 3 are most likely associated with the enzyme active site's opening up to release the product into the solution. Loosely bound domains 1 and 3 have 54% and 18% relative population, respectively, and tightly bound domain 2 has 27% relative population (population percentages are calculated for the data that fall within the black circles in Fig. 2). The significant population of domain 2 indicates that even tightly bound conformations have favorable electrostatic interactions and other possible interactions. Plausible explanations could be that (*i*) domain 2 represents intermediate conformational states of the enzyme in the final product-releasing step while waiting for the right orientation of the amino acid residues necessary to open the active site for product release, thereby populating loosely bound domain 1 and 3, and (*ii*) domains 1 and 3 are populated as parallel pathways along with domain 2 to release the product. The presence of tightly bound states (domain 2) suggests that the product is expelled from the active site into the solution. The existence of both loose states (domain 1 and 3) and a tightly bound state (domain 2) suggests complex conformational dynamics of the active site before the product diffuses away. Although the 2D joint histogram successfully unravels the existence of structurally distinct multiple forms of the active site in the product-releasing step, the low time resolution of our experimental setup limits us from revealing the sequence of appearance of the intermediate conformations in the falling edges of the photon bursts. High time resolution and further structural studies are required to validate a definite conclusion. The corresponding 2D joint distributions of lifetime and rotational correlation time at the rising edge, ON state, and falling edge are shown in Fig. 2 *A1–C1*, respectively. Consistent with 2D joint distribution of lifetime and anisotropy, 2D joint distribution of lifetime and rotational correlation time also shows complex multiple conformational populations in the falling edge.

The formation of a distinct intermediate conformational state in the product release step has also been reported recently. A study with lysozyme showed that an intermediate "unlocked" state is populated to facilitate product release and large-scale conformational fluctuations exist along the catalytic cycle modulating the interaction with the product necessary for releasing it (15). Further, a recent study revealed that dihydrofolate reductase from *Escherichia coli* releases product in two parallel pathways, an intrinsic pathway and an allosteric pathway, and the enzyme's conformational dynamics plays a critical role in controlling product release (16). Experimentally observed continual change in the coupled protein–water hydrogen-bond dynamics during catalytic cycle further supports our finding that different conformational intermediates are formed during a catalytic cycle (10, 43).

To acquire deeper insight about active-site conformational fluctuation during a catalytic event, we characterized the effect of mechanical perturbation on the conformational dynamics. For that purpose we used magnetic tweezers applying a pulling force of ∼2 pN. Although the applied force is much weaker than the force needed to break a hydrogen bond (6–9 pN), previous reports suggest that the 1- to 2-pN external pulling force can deform or unfold an enzyme by 30–100%, thereby weakening the enzyme–substrate interaction (20, 44) (see *Supporting Information* for the force calibration curve). Fig. 3 *A–C* shows the 2D joint distribution of lifetime and anisotropy at the rising edges, during the ON states, and at the falling edges from 356 catalytic events under the magnetic pulling force of ∼2 pN. The rising edge centers on $\tau_f = 3.4 \pm 0.10$ ns, $r = 0.12 \pm 0.06$ and the corresponding τ_r is 2.1 ns. The ON state is centered on $\tau_f = 3.5 \pm 0.14$ ns, $r = 0.12 \pm 0.04$ and the corresponding τ_r is 2.1 ns. Interestingly, falling edge under 2-pN magnetic pulling force consists of only a single domain centering on $\tau_f = 3.5 \pm 0.2$ ns, $r = 0.07 \pm 0.04$, and corresponding τ_r is 1.0 ns. Additionally, the domain at the falling edge centers on lower anisotropy, hence the lower rotational correlation time than that at the rising edge or ON state. The 1.0-ns rotational correlation time at the falling edge under force pulling matches with the rotational correlation time of domains 1 and 3 of the falling edge under no force pulling. This suggests that under force manipulation the enzyme undergoes conformational deformation and loses its native active-site thermal conformational fluctuation to a certain extent. Upon losing its rigid active-site structure the enzyme ceases to have a distinct tightly bound conformational population like domain 2 under no force pulling. At this conjecture, it is important to note that conformational fluctuation of the enzymatic active site due to thermal fluctuation has a critical role in enzymatic activity. As a result of that fluctuation the enzyme will still be able to explore all other subsets of active-site conformations even after being perturbed by a piconewton external pulling force. However, as can be seen from Fig. 3*C*, the clear separation between the conformational domains seen in Fig. 2*C* is lost under the force-pulling condition and the distribution centers on a lower rotational correlation time (1.0 ns). It is well known that enzyme interacts with the transition state much more tightly than the substrate or the product (45). Because we have applied a much weaker pulling force (∼2.0 pN) than that needed to break a hydrogen bond, we expect that the interaction of the product with the active site at the rising edge and ON state remains much stronger and hence unaffected by the piconewton external pulling force. The high rotational correlation time at the rising edge and ON state under force pulling (∼2.0 ns) corroborates this. However, at the falling edge when the enzyme is ready to release the product the interaction further weakens due to the pulling force and the loosely bound state becomes the dominant product-releasing state, which is reflected by faster rotational anisotropy.

A central conjecture in enzymology is that the efficiency of catalysis is mainly directed by the strong structural interaction between enzyme and substrate. However, recent experimental developments reveal significant effects of conformational dynamics on enzymatic reaction rate (2, 4–7). Considering our experimental findings that multiple conformational states are populated during the product release step, we anticipate that the charge redistribution in an enzymatic reaction, as seen in X-ray crystallography (27), may trigger dramatic conformational changes in the enzyme active site, which also can be seen in Fig. 2*C*.

The multiple conformations populated due to the effective charge redistribution facilitate release of the product from the active site either by opening the active site after exploring tightly bound states or by populating multiple parallel pathways where the product is expelled from a tightly bound active site along with a loosely bound open active site. Under a piconewton external

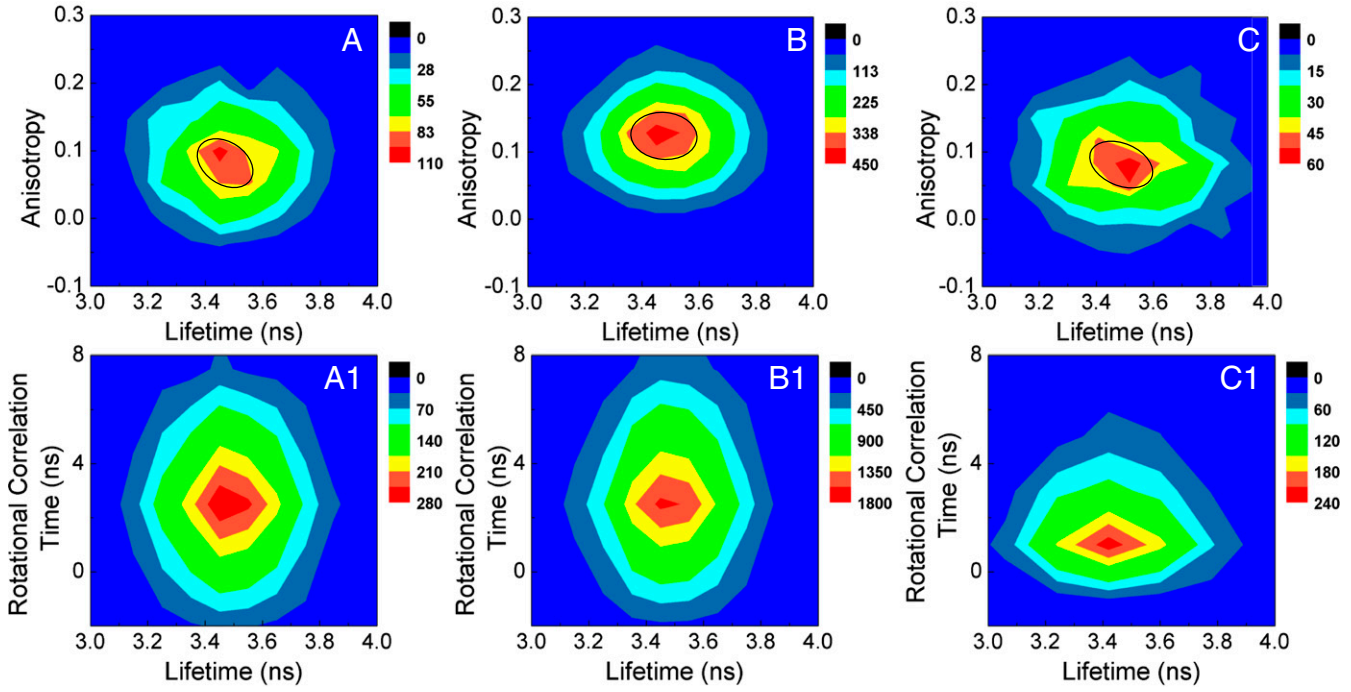

Fig. 3. Two-dimensional joint distribution of anisotropy and lifetime (*Upper*) and rotational correlation time and lifetime (*Lower*) calculated from 356 catalytic turnovers under ~2 pN of magnetic pulling force. Two-dimensional joint distribution of anisotropy and lifetime at (*A*) the rising edge, (*B*) ON state, and (*C*) the falling edge. Two-dimensional joint distribution of rotational correlation time and lifetime at (*A1*) the rising edge, (*B1*) ON state, and (*C1*) the falling edge.

pulling force HRP retains its activity but loses the complex conformational dynamics in the product-releasing step. Interestingly, even after structure deformation, HRP retains its wild-type (or unperturbed) conformational dynamics to a large extent that rely on flexibility. A conceptual representation in Fig. 4 illustrates our finding that the external mechanical force changes not only the enzymatic reaction activity but also the mechanism (i.e., the pathway of the enzymatic reaction).

Conclusion

We have presented a study of HRP conformational dynamics and mechanism during catalysis of oxidation of Amplex Red, demonstrating that a piconewton mechanical force manipulation is able not only to change the enzymatic active-site conformations but also to manipulate the enzymatic reaction pathways. Magnetic tweezers combined with TIRFM-guided SM photon time-stamping spectroscopy has been used to recognize different intermediate conformational states during a catalytic cycle. Our unique approach of using a fluorogenic product and detailed analysis of different catalytic steps of product formation and release gives us the advantage of identifying conformational changes directly associated with enzymatic reaction in real time with single-turnover resolution. The study demonstrated that although the active site populates a single conformation with large-scale fluctuations at the nascent product formation, the conformational dynamics becomes more complex at the product-releasing step. The product-releasing process involves, alongside an open active-site conformational state, distinct tightly bound intermediate states right at the nascent product release from the enzymatic active site, showing parallel product solvation and releasing pathway and product spilling-out pathway. The presence of multiple conformational states and pathways in the product-releasing step indicates that the mechanism by which product exits the active site is much more complex than what has been reported so far. Observing a comparatively simpler conformational population when the enzyme is mechanically perturbed by a piconewton mechanical force further supports this conclusion. Although further experimental, structural, and simulation studies are necessary to draw a generalized picture about the product release mechanism, the insightful information obtained in this study can be significantly useful in understanding the enzymatic reaction mechanism and the related free energy landscape.

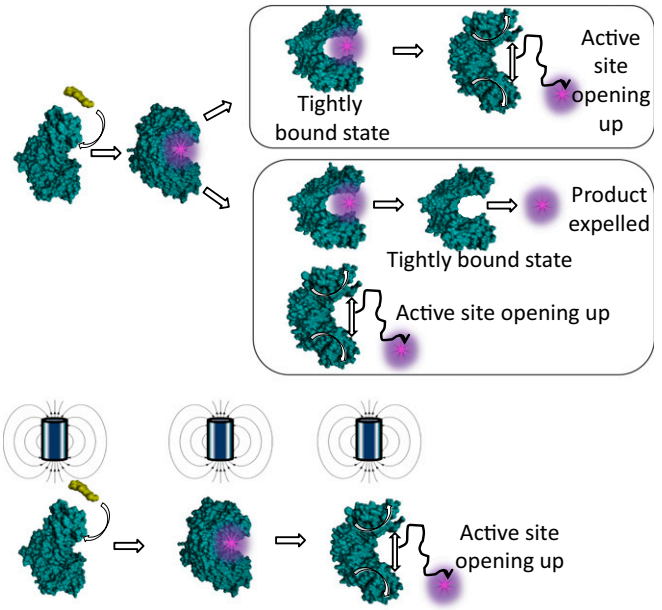

Fig. 4. Schematic representation of the product-releasing pathways.

Materials and Methods

Materials. The HRP-catalyzed reaction converts nonfluorescent Amplex Red into fluorescent resorufin in the presence of H_2O_2. In our system, streptavidin-coated paramagnetic beads were covalently linked to the HRP enzymes through a biotin–streptavidin link.

Sample Preparation. Maleimide-activated HRP was linked to the sulfhydryl (–SH) group of the silanated glass coverslip. HRP has six lysine residues. The -NHS end of the linker NHS-PEG_{12}-biotin reacts with the -NH_2 group of lysine residues. Next, biotin binds with streptavidin coated on the paramagnetic beads. The reaction solution with 200 nM Amplex Red and 2 mM H_2O_2 in PBS buffer (pH 7.4) was prepared just before the experiment (see *Supporting Information* for details).

Experimental Setup. We used a home-built TIRFM-guided confocal fluorescence spectroscope combined with magnetic tweezers based on an inverted microscope (Axiovert 200M; Carl Zeiss) equipped with a 63× oil-immersion objective (N.A. 1.4, Plan-Apochromat; Zeiss). The TIRFM mode helps us to pinpoint spatially randomly distributed enzymes from stochastic fluorescence bursts originating from catalytic events and the confocal mode is used to acquire photon time-stamping data. We acquired SM data while simultaneously applying a pulling magnetic force via magnetic tweezers. Cover glass tethered with HRP was attached at the bottom of the sample chamber and a lid was placed on the top of the chamber to prevent evaporation during data acquisition (see *Supporting Information* for details).

ACKNOWLEDGMENTS. This work was supported by the NIH, National Institute of General Medical Sciences, and the Ohio Eminent Scholar Endowment.

1. Johnson KA (2013) A century of enzyme kinetic analysis, 1913 to 2013. *FEBS Lett* 587(17):2753–2766.
2. English BP, et al. (2006) Ever-fluctuating single enzyme molecules: Michaelis-Menten equation revisited. *Nat Chem Biol* 2(2):87–94.
3. Segel IH (1993) *Enzyme Kinetics: Behavior and Analysis of Rapid Equilibrium and Steady State* (Wiley, New York).
4. Benkovic SJ, Hammes GG, Hammes-Schiffer S (2008) Free-energy landscape of enzyme catalysis. *Biochemistry* 47(11):3317–3321.
5. Edman L, Földes-Papp Z, Wennmalm S, Rigler R (1999) The fluctuating enzyme: A single molecule approach. *Chem Phys* 247(1):11–22.
6. Henzler-Wildman KA, et al. (2007) Intrinsic motions along an enzymatic reaction trajectory. *Nature* 450(7171):838–844.
7. Lu HP, Xun L, Xie XS (1998) Single-molecule enzymatic dynamics. *Science* 282(5395): 1877–1882.
8. Blank K, De Cremer G, Hofkens J (2009) Fluorescence-based analysis of enzymes at the single-molecule level. *Biotechnol J* 4(4):465–479.
9. Zheng D, Lu HP (2014) Single-molecule enzymatic conformational dynamics: Spilling out the product molecules. *J Phys Chem B* 118(31):9128–9140.
10. Dielmann-Gessner J, et al. (2014) Enzymatic turnover of macromolecules generates long-lasting protein-water-coupled motions beyond reaction steady state. *Proc Natl Acad Sci USA* 111(50):17857–17862.
11. Guha S, et al. (2005) Slow solvation dynamics at the active site of an enzyme: Implications for catalysis. *Biochemistry* 44(25):8940–8947.
12. Cao J (2011) Michaelis-Menten equation and detailed balance in enzymatic networks. *J Phys Chem B* 115(18):5493–5498.
13. Wang Y, Gan L, Wang E, Wang J (2013) Exploring the dynamic functional landscape of adenylate kinase modulated by substrates. *J Chem Theory Comput* 9(1):84–95.
14. Sierks MR, Sico C, Zaw M (1997) Solvent and viscosity effects on the rate-limiting product release step of glucoamylase during maltose hydrolysis. *Biotechnol Prog* 13(5):601–608.
15. De Simone A, Aprile FA, Dhulesia A, Dobson CM, Vendruscolo M (2015) Structure of a low-population intermediate state in the release of an enzyme product. *eLife* 4:1–13.
16. Oyen D, Fenwick RB, Stanfield RL, Dyson HJ, Wright PE (2015) Cofactor-mediated conformational dynamics promote product release from Escherichia coli dihydrofolate reductase via an allosteric pathway. *J Am Chem Soc* 137(29):9459–9468.
17. Muddana HS, Sengupta S, Mallouk TE, Sen A, Butler PJ (2010) Substrate catalysis enhances single-enzyme diffusion. *J Am Chem Soc* 132(7):2110–2111.
18. Riedel C, et al. (2015) The heat released during catalytic turnover enhances the diffusion of an enzyme. *Nature* 517(7533):227–230.
19. Golestanian R (2015) Enhanced diffusion of enzymes that catalyze exothermic reactions. *Phys Rev Lett* 115(10):108102.
20. Guo Q, He Y, Lu HP (2015) Interrogating the activities of conformational deformed enzyme by single-molecule fluorescence-magnetic tweezers microscopy. *Proc Natl Acad Sci USA* 112(45):13904–13909.
21. Lippitz M, Erker W, Decker H, van Holde KE, Basché T (2002) Two-photon excitation microscopy of tryptophan-containing proteins. *Proc Natl Acad Sci USA* 99(5):2772–2777.
22. Ehrl BN, Liebherr RB, Gorris HH (2013) Single molecule kinetics of horseradish peroxidase exposed in large arrays of femtoliter-sized fused silica chambers. *Analyst (Lond)* 138(15):4260–4265.
23. Gorris HH, Walt DR (2009) Mechanistic aspects of horseradish peroxidase elucidated through single-molecule studies. *J Am Chem Soc* 131(17):6277–6282.
24. Hassler K, et al. (2007) Dynamic disorder in horseradish peroxidase observed with total internal reflection fluorescence correlation spectroscopy. *Opt Express* 15(9): 5366–5375.
25. Zheng D, Kaldaras L, Lu HP (2012) Total internal reflection fluorescence microscopy imaging-guided confocal single-molecule fluorescence spectroscopy. *Rev Sci Instrum* 83(1):013110.
26. Stirnemann G, Kang SG, Zhou R, Berne BJ (2014) How force unfolding differs from chemical denaturation. *Proc Natl Acad Sci USA* 111(9):3413–3418.
27. Berglund GI, et al. (2002) The catalytic pathway of horseradish peroxidase at high resolution. *Nature* 417(6887):463–468.
28. Veitch NC (2004) Horseradish peroxidase: A modern view of a classic enzyme. *Phytochemistry* 65(3):249–259.
29. Carlsson GH, Nicholls P, Svistunenko D, Berglund GI, Hajdu J (2005) Complexes of horseradish peroxidase with formate, acetate, and carbon monoxide. *Biochemistry* 44(2):635–642.
30. Henriksen A, et al. (1998) Structural interactions between horseradish peroxidase C and the substrate benzhydroxamic acid determined by X-ray crystallography. *Biochemistry* 37(22):8054–8060.
31. He Y, Lu M, Lu HP (2013) Single-molecule photon stamping FRET spectroscopy study of enzymatic conformational dynamics. *Phys Chem Chem Phys* 15(3):770–775.
32. Lu M, Lu HP (2014) Probing protein multidimensional conformational fluctuations by single-molecule multiparameter photon stamping spectroscopy. *J Phys Chem B* 118(41):11943–11955.
33. Rothwell PJ, et al. (2003) Multiparameter single-molecule fluorescence spectroscopy reveals heterogeneity of HIV-1 reverse transcriptase:primer/template complexes. *Proc Natl Acad Sci USA* 100(4):1655–1660.
34. Batista MRB, Martínez L (2013) Dynamics of nuclear receptor Helix-12 switch of transcription activation by modeling time-resolved fluorescence anisotropy decays. *Biophys J* 105(7):1670–1680.
35. Gustavsson T, et al. (2003) Rotational diffusion of the 7-diethylamino-4-methylcoumarin C1 dye molecule in polar protic and aprotic solvents. *Photochem Photobiol Sci* 2(3):329–341.
36. Horng ML, Gardecki JA, Maroncelli M (1997) Rotational dynamics of coumarin 153: Time-dependent friction, dielectric friction, and other nonhydrodynamic effects. *J Phys Chem A* 101(6):1030–1047.
37. Zhao B, Summers FA, Mason RP (2012) Photooxidation of Amplex Red to resorufin: Implications of exposing the Amplex Red assay to light. *Free Radic Biol Med* 53(5): 1080–1087.
38. Edman L, Rigler R (2000) Memory landscapes of single-enzyme molecules. *Proc Natl Acad Sci USA* 97(15):8266–8271.
39. Northrup SH, Erickson HP (1992) Kinetics of protein-protein association explained by Brownian dynamics computer simulation. *Proc Natl Acad Sci USA* 89(8):3338–3342.
40. Nie S, Chiu DT, Zare RN (1994) Probing individual molecules with confocal fluorescence microscopy. *Science* 266(5187):1018–1021.
41. Widengren J, et al. (2006) Single-molecule detection and identification of multiple species by multiparameter fluorescence detection. *Anal Chem* 78(6):2039–2050.
42. Kurnikova MG, Balabai N, Waldeck DH, Coalson RD (1998) Rotational relaxation in polar solvents. Molecular dynamics study of solute-solvent interaction. *J Am Chem Soc* 120(24):6121–6130.
43. Grossman M, et al. (2013) Correlated structural kinetics and retarded solvent dynamics at the metalloprotease active site. *Nature* 18(9):1199–1216.
44. Guo Q, He Y, Lu HP (2014) Manipulating and probing enzymatic conformational fluctuations and enzyme-substrate interactions by single-molecule FRET-magnetic tweezers microscopy. *Phys Chem Chem Phys* 16(26):13052–13058.
45. Pauling L (1946) Molecular architecture and biological reactions. *Chem Eng News* 10: 1375–1376.